Research on a Novel Vibration Evaluation of Motorbike's Suspension Using Multi-body Dynamic Model under Different Road Surfaces

Ngoc Dai Pham
Lecturer
Department of Automotive Engineering
Faculty of Transportation Engineering, Ho Chi Minh City University of Technology (HCMUT) – Vietnam National University Ho Chi Minh City, 268 Ly Thuong Kiet Street District 10, Ho Chi Minh City
Vietnam

This study has contributed a new method in analyzing the vibration responses of a motorbike suspension with damping ratio ξ_s using a multi-body dynamic model (MBD). The special feature of this method is that the MBD model can represent the system's behaviors without establishing dynamic equations. This method requires establishing tight kinematic constraints between the model's elements in the XY plane at the connection positions such as road - wheel, wheel - guiding element - suspension - motor's frame in Matlab Simmechanics environment. The results are evaluated based on various response indices such as acceleration, relative displacement, road holding ability, and comfort level according to the cases of operating under harmonic, transient, and random excitations. The MBD model responses in operating cases tends to be consistent with reality and can be applied in the design process of motorcycle suspension based on the evaluation of the influences of ξ_s.

Keywords: *Motorbike, Multi-Body Dynamic, Transient, Harmonic, Random, ISO 2631:1-1997, Comfort*

1. INTRODUCTION

Drivers are always affected by vibrations transmitted from the vehicle to the body during operation [1,2]. Vibrations mainly originate from the vehicle moving on rough roads, engine and inertia vibrations of the continuous speed change process [3]. Researchers have long recognized the effects of vibrations on the comfort level, health and work efficiency of people sitting in the vehicle [4]. The suspension system with elastic elements - shock absorbers can store energy and release energy, thus contributing to reducing vehicle body vibration when the vehicle is stimulated [5]. The vehicle suspension system comprises 05 main elements, including sprung mass, unsprung mass, elastic element, shock absorber and guiding elements [6]. The function of the elastic element is to absorb vibration energy and convert it into elastic potential energy. The shock absorbers convert the absorbed energy into heat energy and transmit it to the outside environment [7]. The guiding element connects the suspension system to the vehicle frame, ensuring that the system deforms in the design direction and transmits the traction force from the road surface to the vehicle body [7]. However, during operation, the vibration isolation efficiency of the suspension system under different working conditions is different [8]. Accordingly, corresponding to the road surface profile types and the speed of movement on it, the behaviour of the vehicle body and the driver is also different in terms of *displacement* and acceleration values [9]. Study on the influence of vehicle suspension system parameters on the oscillation dynamics of the vehicle body in the vertical and horizontal directions [10]. Application of a new design method with matrix inequalities and passivity constraints for the suspension system to ensure the wheel's ability to grip the road in the horizontal direction [11]. Study to evaluate the possibility of applying a hybrid suspension system to a 2-wheel vehicle with integrated elastic elements - shock absorbers [12].

Passive suspension systems on vehicles or seats in general and motorcycle suspension systems, in particular, all have the problem of not achieving the optimal state of acceleration and displacement simultaneously [13]. Therefore, suspension systems that combine a damper control system (semi-active) or are equipped with an auxiliary system that creates a direct intervention force (active) have been studied. Semi-active suspension systems mainly adjust the structural parameters of the existing system without creating additional external forces or moments that cause changes in the behaviour state [14,15]. In particular, experimental research determines electromagnetic damping parameters and applies them to motorcycles' semi-active rear suspension systems [14]. In addition, research on typical semi-active suspension systems can include the integration of 02 controllers in the front and rear suspension into the entire vehicle model, which are continuously adjusted by the central controller [15]. Similar to the automatic suspension system on automobiles [16], the active support system is also applied to the suspension system of motorbikes. Automatic suspension systems can be mentioned as research on applying electronic control systems to adjust the initial deformation state corresponding to the vehicle load [17,18].

Received: February 2025, Accepted: June 2025
Correspondence to: Ngoc Dai Pham, Faculty of Transportation Engineering, University of Technology, 268 Ly Thuong Kiet Street, District 10, Ho Chi Minh City, Vietnam. E-mail: phamngocdai@hcmut.edu.vn
doi: 10.5937/fme2503386D

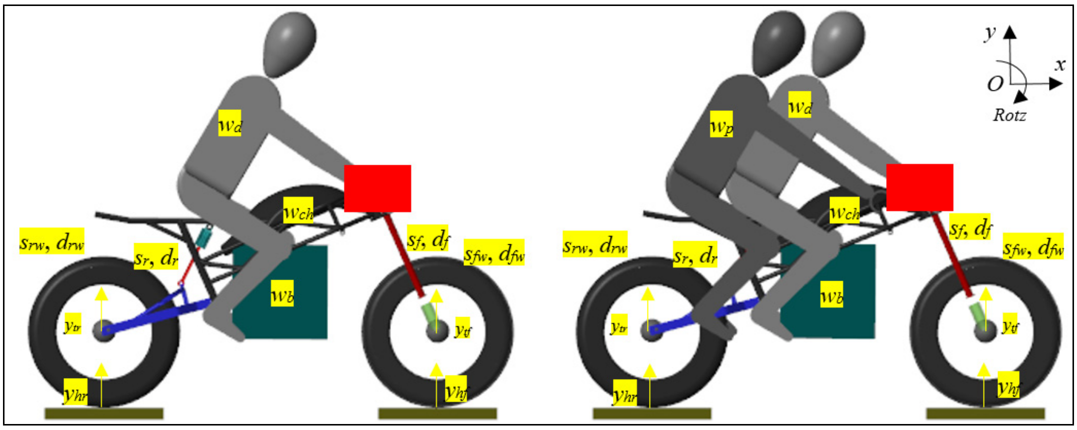

Figure 1. Matlab Simmechanics model in the simulation environment

Currently, modelling vehicle suspension systems, especially passenger vehicles and motorcycles, is of interest to various analytical models [14,15]. With mo–torcycle suspension systems, the system's nonlinearity is mainly in the damping element, so to increase the accu–racy of the evaluation model, asymmetric linear or non–linear damping models are proposed [19]. The com–monly used models for evaluating the effectiveness of suspension systems are 02 degrees of freedom, which only considers vertical vibrations, and 04 degrees of freedom, which considers vertical vibrations and pitch motion [10,14,15].

Using a simple model such as 02 degrees of freedom does not consider the influence of the pitch motion of the vehicle body, so it does not fully respond to reality. Eliminating the directional mechanism dynamic influence for simple 4DOF models affects the overall acceleration and displacement values, leading to an uncertain evalu–ation result. In addition, considering only the operating conditions of a single vehicle for a specific vehicle type does not provide enough data for application in many practical operating conditions. From the above limita–tions, the study applied a multi-body dynamic model to ensure the model structure, thereby ensuring the influence of the degrees of freedom of the vehicle body and applicability in many practical working conditions. This method of building a multi-body dynamic model can be applied to the design process in calculation to select the technical parameters of elastic elements - shock absorbers of motorbike suspension systems according to each specific operating case in practice. In addition, the obta–ined simulation results can be used to adjust the available passive suspension system parameters according to the above operating cases to ensure optimal response accor–ding to the requirements of the occupants.

2. ANALYSIS MODEL AND TECHNICAL PARA–METERS

2.1 Matlab Simmechanics model

The simulation model in Figure 1 is built to ensure the movements according to the corresponding degrees of freedom in the *xOy* plane, including displacements in the two directions, *Ox* and *Oy*, and rotating around the *Oz* axis. This is done through the realistic description of The connections between the mass elements of the vehicle such as the frame, guiding mechanism (swing arm), wheels, etc. The degrees of freedom between the objects are constrained according to Table 1.

Table 1. Joints' constraint

Element 1	Element 2	*x*	*y*	*Rotz*
Front wheel	Road	x	x	x
Rear wheel	Road	x	x	x
Swing arm	Wheel	-	-	x
Swing arm	Frame	-	-	x
Rear cylinder	Swing arm	-	-	x
Rear piston	Frame	-	-	x
Front cylinder	Wheel	-	-	x
Front piston	Frame	-	-	-

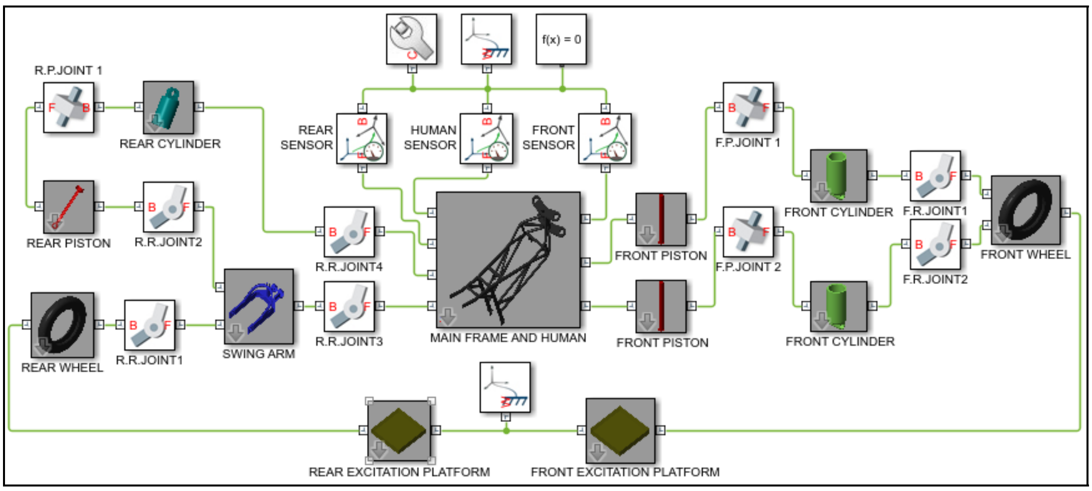

Figure 2. Connection diagram of simscape model's elements

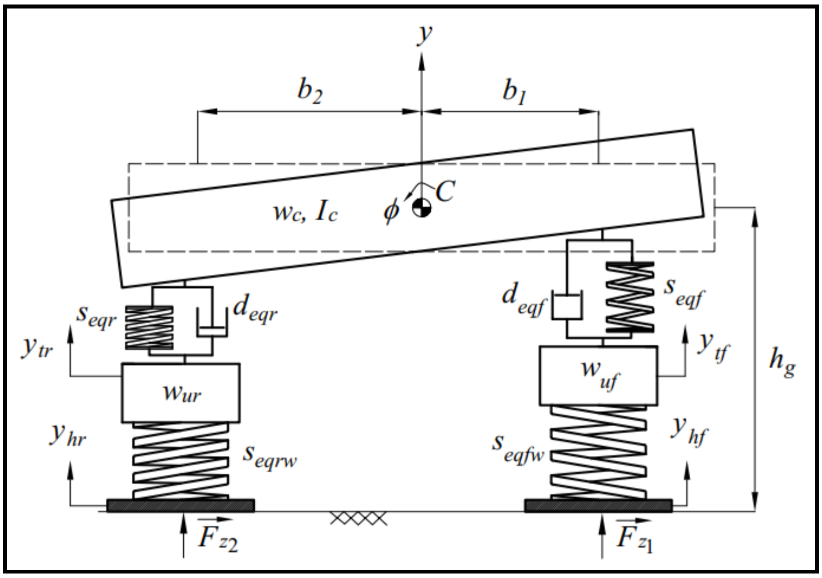

Figure 3. Motorbike 4DOF model

Table 2. Joints between elements

Element 1	Element 2	Matlab joint block
Front wheel	Road	2DOF joint
Rear wheel	Road	2DOF joint
Swing arm	Wheel	Revolute joint
Swing arm	Frame	Revolute joint
Rear cylinder	Swing arm	Revolute joint
Rear piston	Frame	Revolute joint
Front cylinder	Wheel	Revolute joint
Front piston	Frame	Fixed
Cylinder	Piston	Prismatic joint
Unsprung mass	Wheel	Prismatic joint

2.2 Theoretical model

The theoretical analysis model, Figure 3, with the technical parameters of the suspension system, the coordinate parameters of the centre of gravity and the survey parameters are converted into a mathematical model. Apply the general form of Lagrange's equation according to (1) to the system of Figure 3.

$$\frac{d}{dt}\left(\frac{\partial K}{\partial \dot{q}_r}\right)-\frac{\partial K}{\partial q_r}+\frac{\partial D}{\partial \dot{q}_r}+\frac{\partial V}{\partial q_r}=f_r \quad (1)$$

The kinetic energy K, potential energy V, and dissi–pation function D of the mechanical system are res–pectively computed as follows.

$$K=\frac{1}{2}w_c\dot{y}^2+\frac{1}{2}w_{uf}\dot{y}_{tf}^2+\frac{1}{2}w_{ur}\dot{y}_{tr}^2+\frac{1}{2}I_c\dot{\phi}^2 \quad (2)$$

$$\begin{aligned}V=&\frac{1}{2}s_{eqfw}\left(y_{tf}-y_{hf}\right)^2+\frac{1}{2}s_{eqrw}\left(y_{tr}-y_{hr}\right)^2+\ldots\\&+\frac{1}{2}s_{eqf}\left(y-y_{tf}-b_1\phi\right)^2+\frac{1}{2}s_{eqr}\left(y-y_{tr}+b_2\phi\right)^2\end{aligned} \quad (3)$$

$$D=\frac{1}{2}d_{eqf}\left(\dot{y}-\dot{y}_{tf}-b_1\dot{\phi}\right)^2+\frac{1}{2}d_{eqr}\left(\dot{y}-\dot{y}_{tr}-b_2\dot{\phi}\right)^2 \quad (4)$$

The differential dynamic equations describe vehicle vibration as (5).

$$[W]\ddot{Y}+[D]\dot{Y}+[S]Y=F \quad (5)$$

$$[W]=\begin{bmatrix} w_c & 0 & 0 & 0\\ 0 & I_c & 0 & 0\\ 0 & 0 & w_{uf} & 0\\ 0 & 0 & 0 & w_{ur}\end{bmatrix}$$

$$[D]=\begin{bmatrix} d_{eqf}+d_{eqr} & b_2d_{eqr}-b_1d_{eqf} & -d_{eqf} & -d_{eqr}\\ b_2d_{eqr}-b_1d_{eqf} & d_{eqf}b_1^2+d_{eqr}b_2^2 & b_1d_{eqf} & -b_2d_{eqr}\\ -d_{eqf} & b_1d_{eqf} & d_{eqf} & 0\\ -d_{eqr} & -b_2d_{eqr} & 0 & d_{eqr}\end{bmatrix}$$

$$[S]=\begin{bmatrix} s_{eqf}+s_{eqr} & b_2s_{eqr}-b_1s_{eqf} & -s_{eqf} & -s_{eqr}\\ b_2s_{eqr}-b_1s_{eqf} & s_{eqf}b_1^2+s_{eqr}b_2^2 & b_1s_{eqf} & -b_2s_{eqr}\\ -s_{eqf} & b_1s_{eqf} & s_{eqf}+s_{eqfw} & 0\\ -s_{eqr} & -b_2s_{eqr} & 0 & s_{eqf}+s_{eqrw}\end{bmatrix}$$

$$\ddot{Y}=\begin{bmatrix}\ddot{y}\\ \ddot{\phi}\\ \ddot{y}_{tf}\\ \ddot{y}_{tr}\end{bmatrix},\dot{Y}=\begin{bmatrix}\dot{y}\\ \dot{\phi}\\ \dot{y}_{tf}\\ \dot{y}_{tr}\end{bmatrix},Y=\begin{bmatrix}y\\ \phi\\ y_{tf}\\ y_{tr}\end{bmatrix},F=\begin{bmatrix}0\\ 0\\ y_{tf}s_{eqfw}\\ y_{tr}s_{eqrw}\end{bmatrix}$$

2.3 Input parameters

2.3.1 Transient excitation $y_t(t)$

Basing on the IRC 99-1988 standard [20], this study calculated transient excitation signal $y_t(t)$ according to (6). With the parameters, d_1 = 3.7 (m), d_2 = 0.1 (m), speed $v \in$ [10, 80] (km/h).

$$y_t(t)=\begin{cases} d_2\sin^2\dfrac{\pi v}{d_1}t; & 0\le t<\dfrac{d_1}{v}\\ 0; & t<0,\ t\ge\dfrac{d_1}{v}\end{cases} \quad (6)$$

The simulation results of the excitation signal at dif–ferent speed cases, including low-speed v = 10 (km/h), medium-speed v = 40 (km/h) and high-speed v = 80 (km/h), are shown in Figure 4.

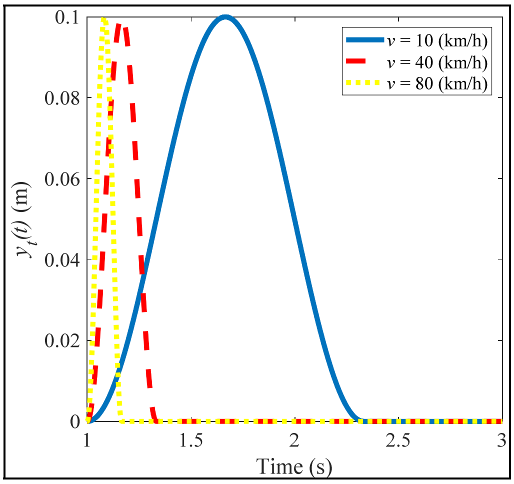

Figure 4. Excitation signal $y_h(t)$ (m)

2.3.2 Harmonic excitation $y_h(t)$

The harmonic excitation signal $y_h(t)$ is simulated in the normal operating frequency range of the suspension system $f \in [0, 15]$ (Hz) [21]. With excitation amplitude $d_2 = 0.005$ (m), cycle length $d_1 = 1$ (m), and vehicle speed $v \in [0, 15]$ (m/s), the value $y_h(t)$ is calculated according to (7).

$$y_h(t) = \frac{d_2}{2}\sin\left(\frac{2\pi v}{d_1}t\right) \tag{7}$$

The simulation results of the excitation signal at different frequency cases $f = [1\ 2\ 3]$ (Hz) are shown in Figure 5.

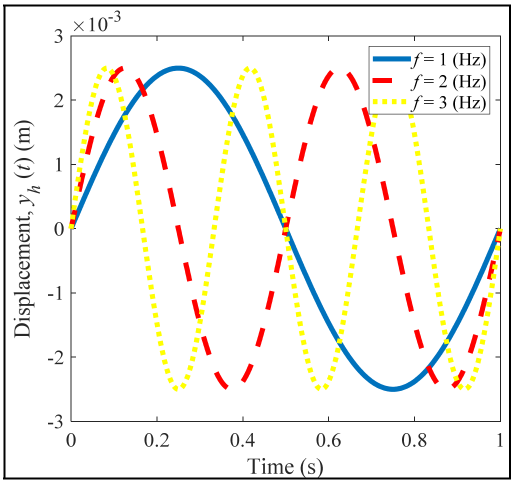

Figure 5. Harmonic excitation $y_h(t)$

2.3.3 Random excitation $y_r(t)$

According to ISO 8608 standard [22], with the number of sine waves chosen $N = 500$, amplitude reduction $w = 2$, at each time t(s) on the measurement time-domain T(s), corresponding to the vehicle speed v (km/h), the road surface excitation value $y_r(t)$ is calculated accor–ding to (8).

$$y_r(t) = \sum_{i=1}^{N}\sqrt{2\Phi_0\left(\frac{\Omega_i}{\Omega_0}\right)^{-w}\Delta\Omega}\,\sin\left(\Omega_i.v.t - \psi_i\right) \tag{8}$$

With:

Ω_i : The wavenumbers

ψ_i: The different sets of distributed phase angles (rad)

Φ_0 : The power spectral density (PSD) at the reference wavenumber $\Omega_0 = 1$ (rad/m)

The $y_r(t)$ signal describes a random road surface with different road quality types. The road surface quality level C is chosen for analysis corresponding to the *PSD* value of $\Phi_{0C} = 8.10^{-6}$ (m^3/rad), Figure 6.

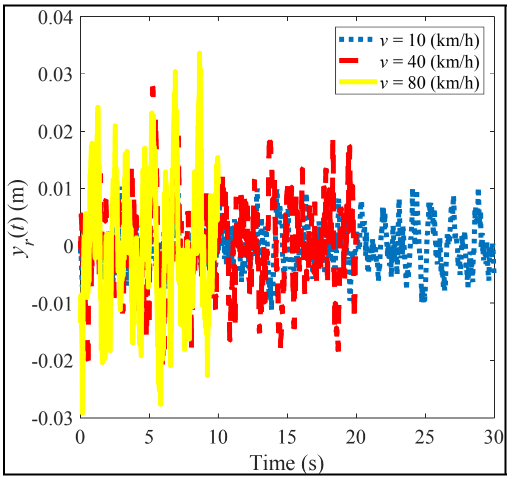

Figure 6. Random excitation $y_r(t)$ [22]

3. EVALUATION CRITERIA

Under transient excitation

The transient excitation signal is used to evaluate the safe deformation of the suspension system, the human body's stability, and the ability to grip the road at the wheel according to TR_{rel}, TR_{acc}, and TR_{TDL} values. When TR_{rel}>100(%), the deformation of the suspension system exceeds the allowable limit and vice versa. For the human body, when TR_{acc}>100(%), the body bounces off the seat, causing instability when driving. Similarly, when TR_{TDL}>100(%), the wheel no longer grips the road, causing unsafety.

Suspension system's relative displacement response TR_{rel} (9).

$$TR_{rel} = \frac{Max\left|x_{Cylinder}(t) - x_{Piston}(t)\right|}{\Delta x_L}.100(\%) \tag{9}$$

Human body vertical acceleration response TR_{acc} (10).

$$TR_{acc} = \frac{Max\left(\ddot{x}_{human}(t)\right)}{g}.100(\%) \tag{10}$$

Tyre dynamic load response TR_{TDL} (11).

$$TR_{TDL} = \frac{Max\left(k_t\left(y_t(t) - y(t)\right) + c_t\left(\dot{y}_t(t) - \dot{y}(t)\right)\right)}{mg}.100(\%) \tag{11}$$

Under harmonic excitation

The harmonic excitation signal is used to evaluate the effect of frequency on the amplitude of the output oscillation signals including the relative displacement of the suspension system HA_{rel} and the body acceleration HA_{acc}. Accordingly, the commonly accepted values of HA_{rel} and HA_{acc} are less than 3 [21].

Suspension system's relative displacement gain response HA_{rel} (12). With $x_{rel} = x_{Cylinder}(t) - x_{Piston}(t)$.

$$HA_{rel} = \frac{Max\left(x_{rel}\right) - Min\left(x_{rel}\right)}{d_2}.100\left(\%\right) \tag{12}$$

Human body vertical acceleration gain response HA_{acc} (13).

$$HA_{acc} = \frac{Max\left|\ddot{x}_{human}\left(t\right)\right|}{0.5d_2\left(2\pi v/d_1\right)^2}.100\left(\%\right) \tag{13}$$

Under random excitation

The random signal is used to evaluate the comfort level of the person subjected to vibration through the overall vibration acceleration value acc_v (m/s^2) according to the guidelines of ISO 2631:1-1997 [4]. The value of acc_v over the entire measured domain T (s) is the Root Mean Square (RMS) of the acceleration values $acc_w(t)$ (m/s^2) at each time t (s), according to (14).

$$acc_v = \sqrt{\frac{1}{T}\int_0^T acc_w^2(t)dt} \tag{14}$$

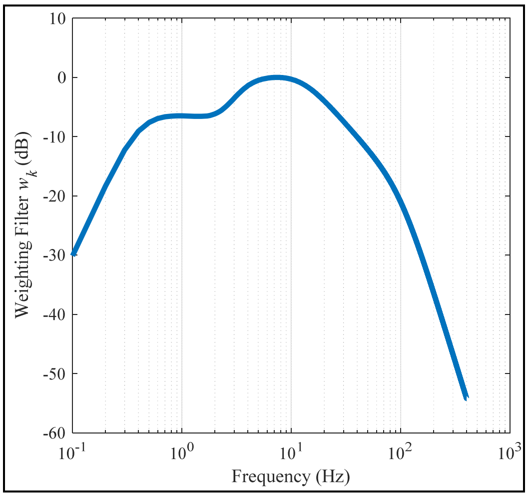

Figure 7. Frequency weighting filters w_k [3]

The acceleration value $a_w(t)$, according to ISO 2631:1-1997, is the value taking into account the influence of frequency on the domain $f_r \in [0.5, 20]$ (Hz) represented by the weighting filter w_k [4], according to (15).

$$w_k = \left|L_{hp}\left(s\right)\right|.\left|L_{lp}\left(s\right)\right|.\left|L_{avt}\left(s\right)\right|.\left|L_{us}\left(s\right)\right| \tag{15}$$

With:

$|L_{hp}(s)|$: High - pass filter (16):

$$\left|L_{hp}\left(s\right)\right| = \sqrt{\frac{f_r^4}{f_r^4 + f_{r1}^4}} \tag{16}$$

$|L_{lp}(s)|$: Low-pass filter (17):

$$\left|L_{lp}\left(s\right)\right| = \sqrt{\frac{f_{r2}^4}{f_r^4 + f_{r2}^4}} \tag{17}$$

$|L_{avt}(s)|$: Acceleration-velocity transition filter (18):

$$\left|L_{avt}\left(s\right)\right| = \sqrt{\frac{f_r^2 + f_{r3}^2}{f_{r3}^2}}\sqrt{\frac{f_{r4}^4.R_4^2}{f_r^4.R_4^2 + f_r^2.f_{r4}^2.\left(1-2R_4^2\right) + f_{r4}^4.R_4^2}} \tag{18}$$

$|L_{us}(s)|$: Upward step filter (19):

$$\left|L_{us}\left(s\right)\right| = \frac{R_6}{R_5}\sqrt{\frac{f_r^4.R_5^2 + f_r^2.f_{r5}^2.\left(1-2R_5^2\right) + f_{r5}^4.R_5^2}{f_r^4.R_5^2 + f_r^2.f_{r5}^2.\left(1-2R_5^2\right) + f_{r6}^4.R_6^2}} \tag{19}$$

Based on the calculated acc_v (m/s^2) value, the vibration comfort level of the person is divided into levels according to Table 3.

Table 3. Driver and passenger uncomfortable feeling level under different acceleration ranges [4]

Acceleration evaluation value acc_v (m/s^2)	Uncomfortable feeling level
$acc_v < 0.31$	Not
$0.31 < acc_v < 0.6$	A little
$0.5 < acc_v < 1$	Fairly
$0.8 < acc_v < 1.6$	Completely
$1.3 < acc_v < 2.5$	Very
$acc_v > 2$	Extremely

4. RESULTS AND DISCUSSION

The simulation results of the time-based cases are summarized in the speed domain (transient, random) and the frequency domain (harmonic). In addition, at each speed and frequency value, the optimal ξ_s value is obtained. From the database of optimal ξ_s values, vehicle users can adjust the damper according to their needs to ensure the most stable vehicle operation according to acceleration condition, relative displacement condition, and wheel traction or avoid the effects of resonance on the frequency domain. In addition, the set of survey results also shows that the cases of carrying 01 people and 02 people sometimes have a significant difference in the optimal ξ_s value. The specific results are presented in the graphs below.

Transient excitation

The typical response values of the human body and vehicle suspension system in the time domain are summarized in Figure 8. The synthesized cases include the case of considering the same average vehicle speed $v = 40$ (km/h), the damping ratio value $\xi_s = [0.2\ 0.5]$ and the case of considering the same damping ratio $\xi_s = 0.5$, the vehicle speed value $v = [40\ 80]$ (km/h). In the first case, when the vehicle moves at an average speed $v = 40$ (km/h), the positive vertical acceleration value with $\xi_s = 0.2$ is more significant than that with $\xi_s = 0.5$. However, the system's stabilization time with $\xi_s = 0.5$ is faster. Similarly, the response values of the pitch angle, the relative displacement of the suspension system, and the dynamic load on the wheel all have the same trend as the acceleration. In the second case, the positive acceleration response value is most significant when the vehicle carries 01 people at v = 80 (km/h) and gradually decreases correspondingly to the case of the vehicle carrying 01 people v = 40 (km/h), the vehicle carrying 02 people v = 80 (km/h). The response value of the pitch angle does not differ much in the cases. For the response of relative displacement and dynamic load at the wheels, the most significant case when the vehicle carries 02 people at v = 80 (km/h) gradually decreases correspondingly to the case of the vehicle carrying 01 people v = 80 (km/h), when the vehicle carrying 02 people v = 40 (km/h).

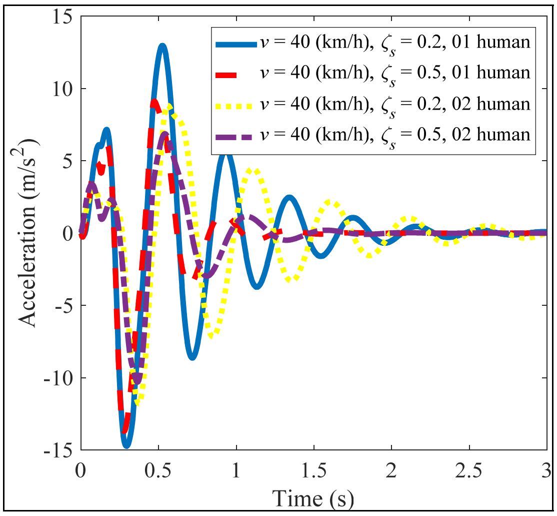

a. Acceleration (m/s^2), v = 40 (km/h)

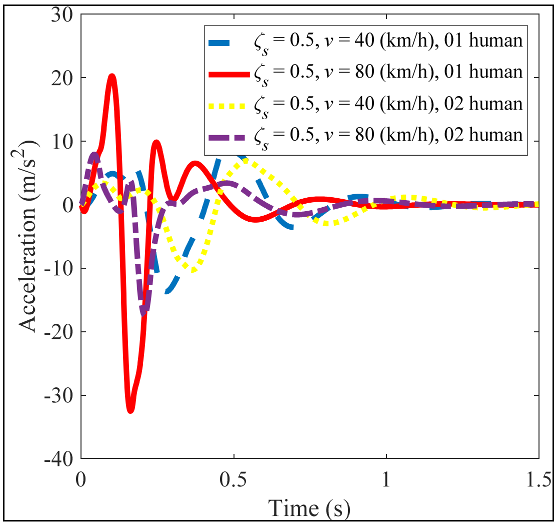

b. Acceleration (m/s^2), ξ_b = 0.5

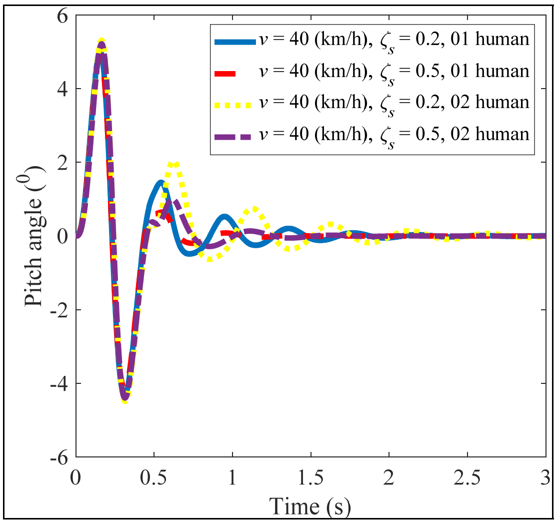

c. Pitch angle (^{o}) , v = 40 (km/h)

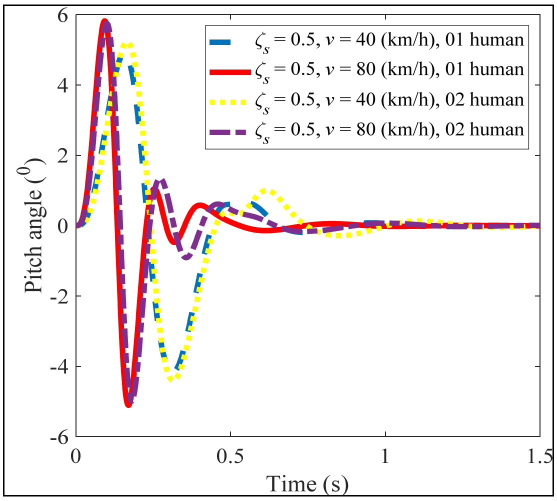

d. Pitch angle (^{o}), ξ_b = 0.5

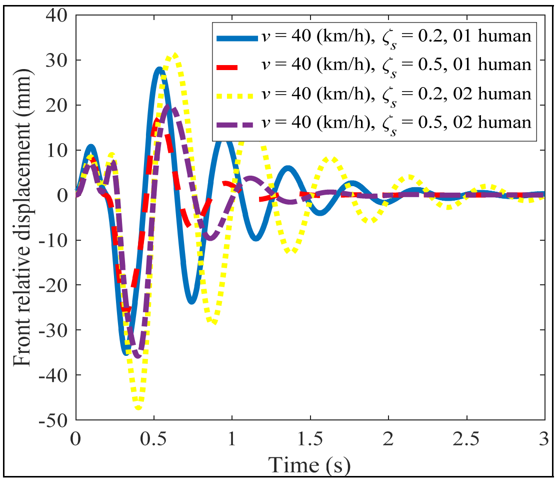

e. Front relative displacement, v = 40 (km/h)

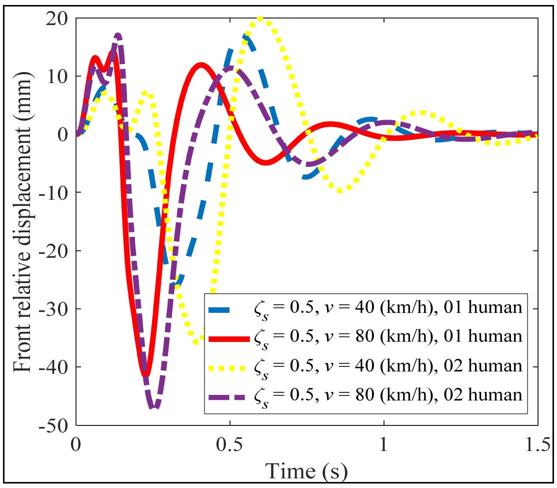

f. Front relative displacement, ξ_b = 0.5

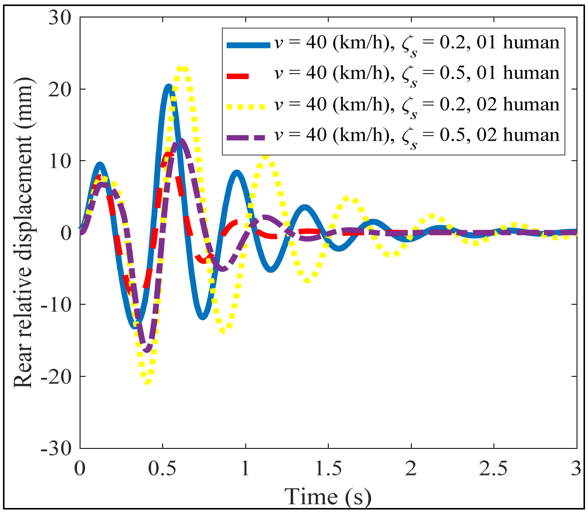

g. Rear relative displacement, *v* = 40 (km/h)

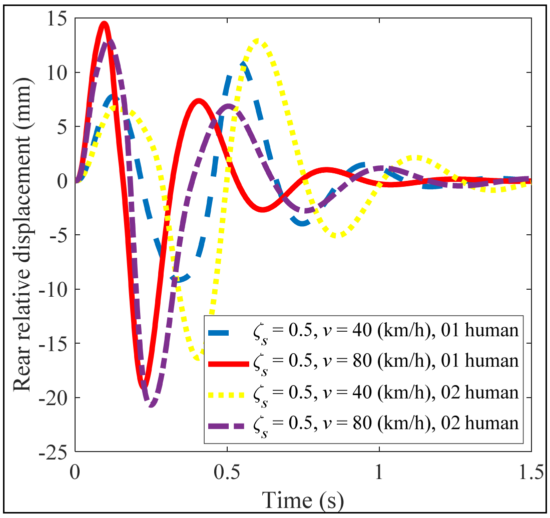

h. Rear relative displacement, ξ_b = 0.5

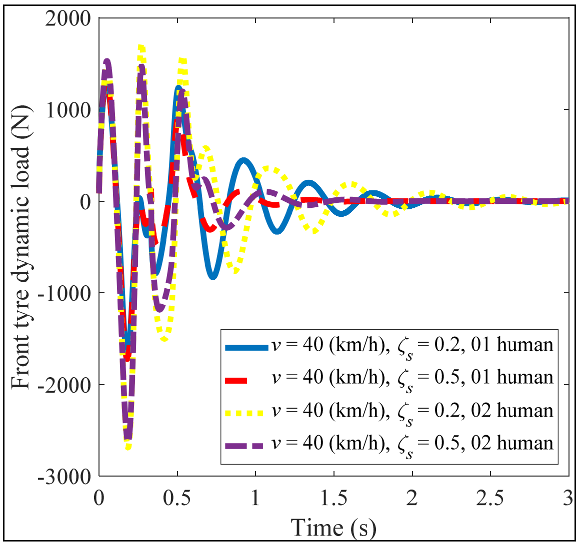

i. Front tyre dynamic load, *v* = 40 (km/h)

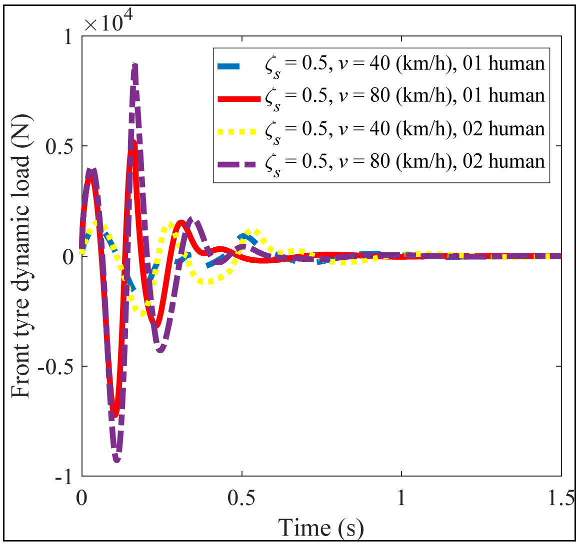

j. Front tyre dynamic load, ξ_b = 0.5

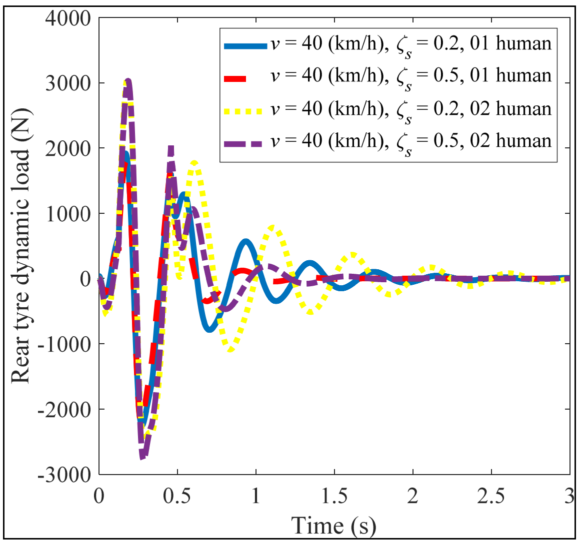

k. Rear tyre dynamic load, *v* = 40 (km/h)

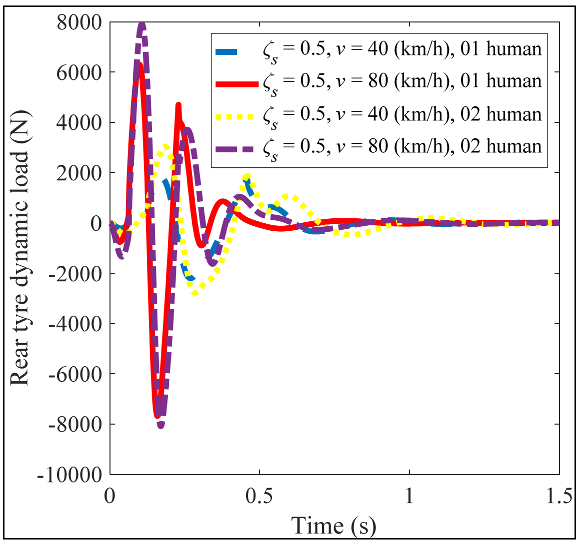

l. Rear tyre dynamic load, ξ_b = 0.5

Figure 8. Transient - Responses in the time domain

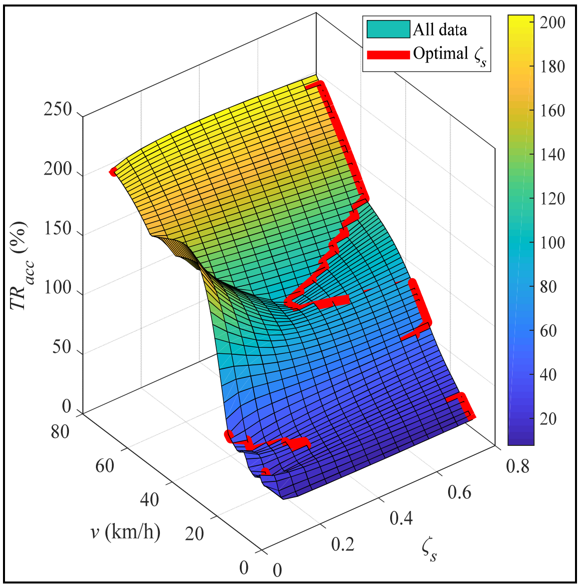

a. ***TR*$_{acc}$ (%) – 01 occupant**

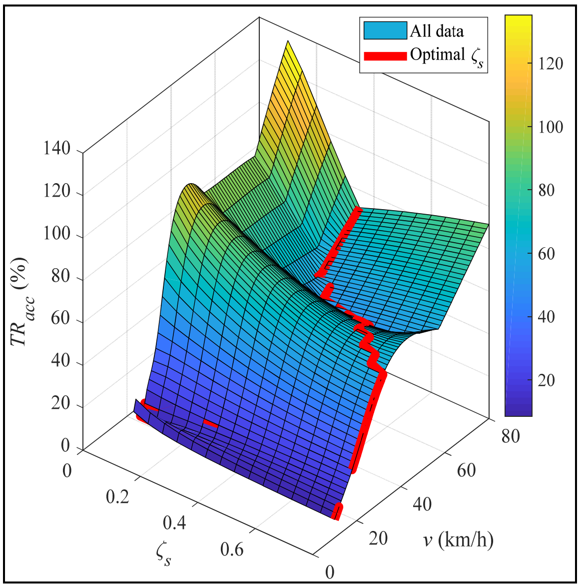

b. ***TR*$_{acc}$ (%) – 02 occupants**

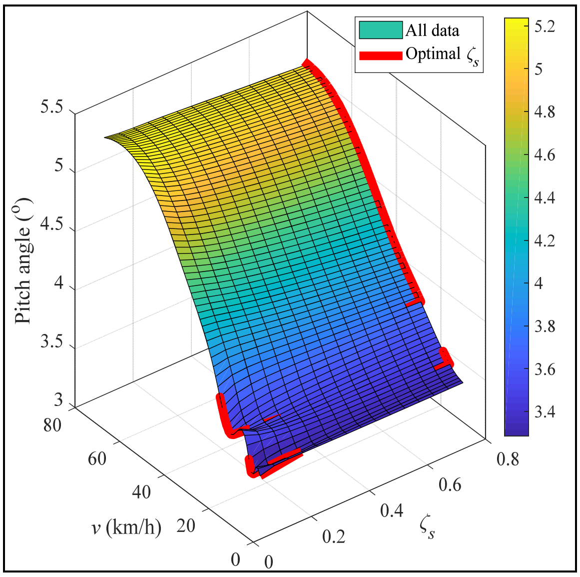

c. Maximum pitch angle (°) – 01 occupant

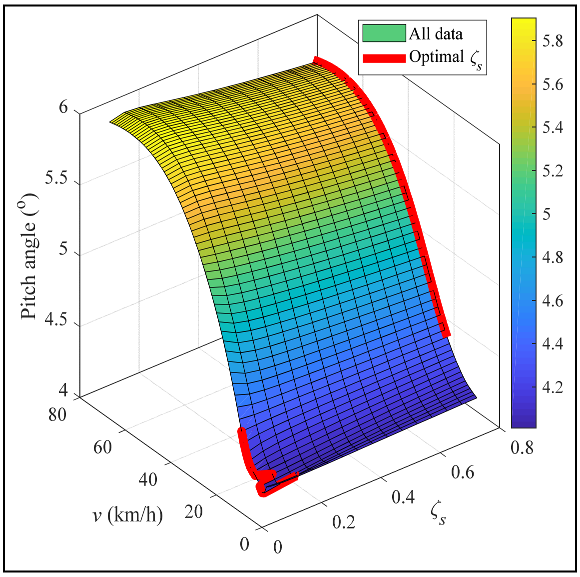

d. Maximum pitch angle (°) – 02 occupants

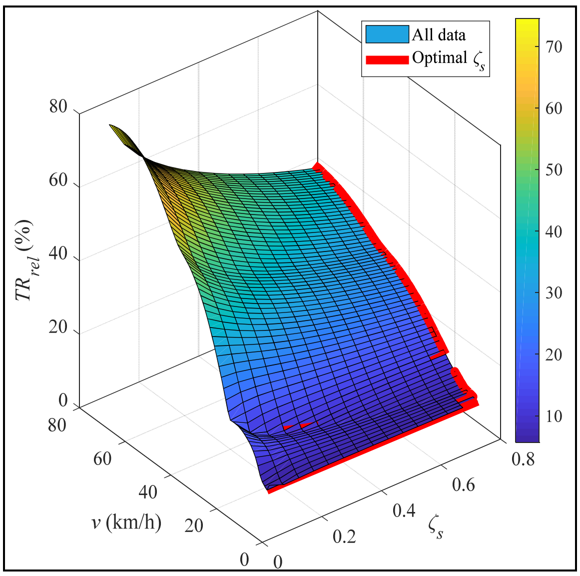

e. Front *TR*$_{rel}$ (%) – 01 occupant

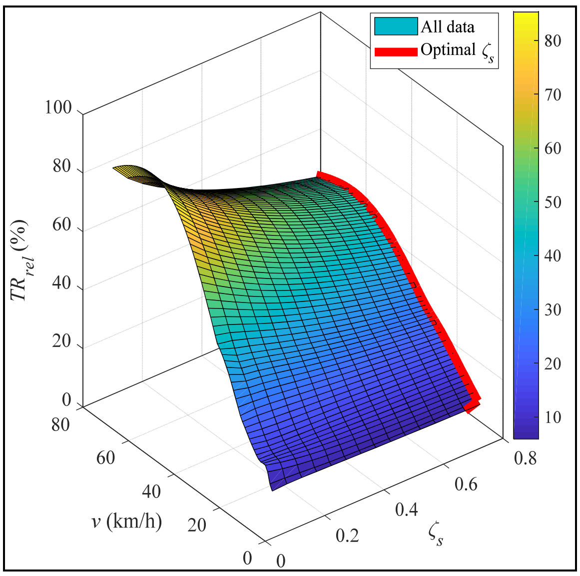

f. Front *TR*$_{rel}$ (%) – 02 occupants

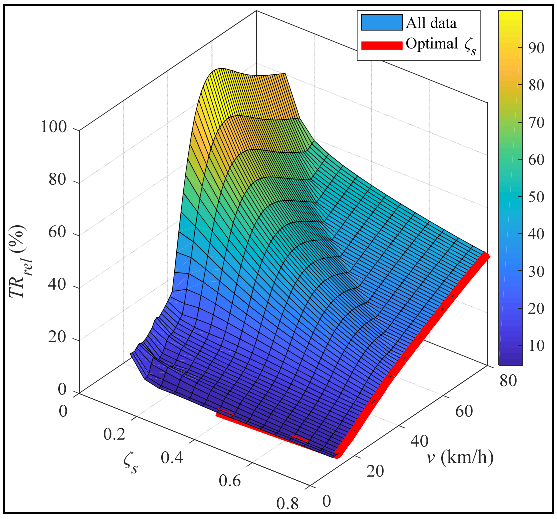

g. Rear TR_{rel} (%) – 01 occupant

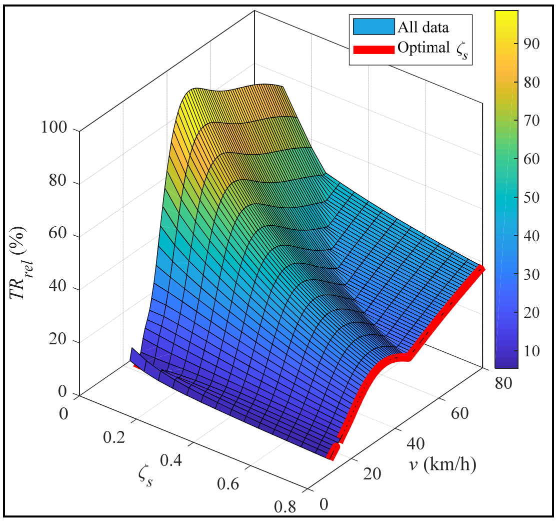

h. Rear TR_{rel} (%) – 02 occupants

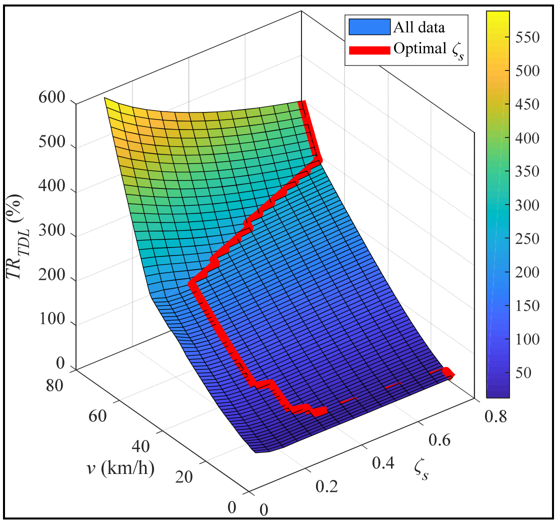

i. Front TR_{TDL} (%) – 01 occupant

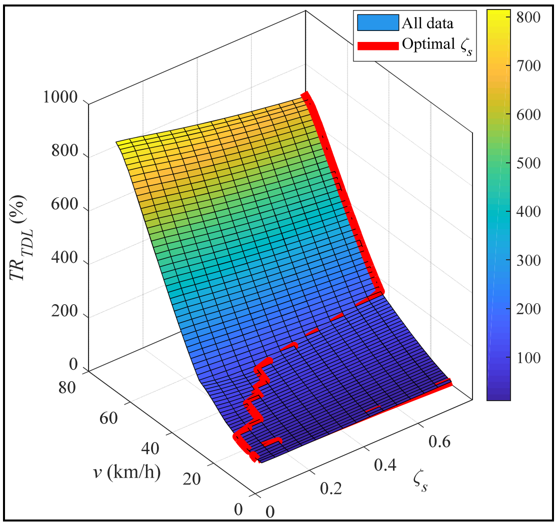

j. Front TR_{TDL} (%) – 02 occupants

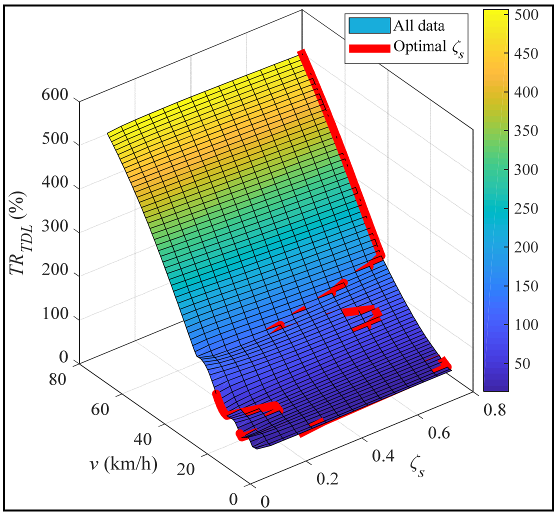

k. Rear TR_{TDL} (%) – 01 occupant

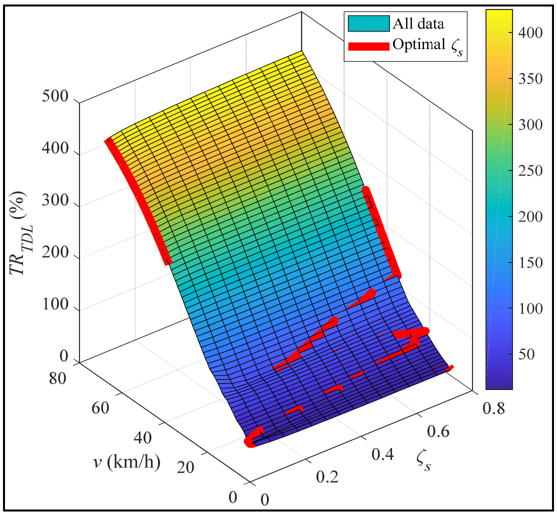

l. Rear TR_{TDL} (%) – 02 occupants

Figure 9. Transient - Responses in the velocity v and damping ratio ξ_s domain

In the case of transient excitation, the maximum response values including maximum acceleration response TR_{acc} (%), maximum pitch angle around the Oy axis response, maximum relative displacement response TR_{rel} (%), maximum dynamic load response at the wheel TR_{TDL} (%) are synthesized and analyzed as Figure 9.

Considering the maximum acceleration response TR_{acc} (%), with the same damping ratio value ξ_s, the TR_{acc} value increases as vehicle speed v (km/h) inc–

reases. However, when considering the same vehicle speed value v (km/h), as increasing ξ_s value, in the region with speed below average v<40 (km/h), the optimal ξ_s value is scattered without any trend. Besides, in the region with an average speed of 40 (km/h)<v<60 (km/h), the optimal ξ_s value has a gradually increasing magnitude and remains constant in the high-speed re–gion v>60 (km/h). For the case of carrying 02 people, the overall TR_{acc} value is distributed in the regions of more significant variation than when carrying 01 per–son. Accordingly, in the low-speed region v<40 (km/h), the optimal ξ_{ss} value is almost entirely distributed in the small value region. In the medium-speed region 40 (km/h)<v<60 (km/h), the optimal ξ_s value decreases from ξ_s = 0.8 to ξ_s = 0.4 and stabilizes at 0.4 in the entire high-speed region v>60 (km/h).

Considering the maximum pitch angle response, the cases of vehicle carrying 01 and 02 people have a similar trend of maximum pitch angle variation. With the same ξ_s value, the pitch angle value increases with the increase in vehicle speed v (km/h). In the low-speed region v<20 (km/h), the maximum pitch angle value is distributed in the small region and vice versa; it is distributed in the large region with vehicle speed v>20 (km/h).

Considering the relative displacement response of the front and rear suspension systems, the TR_{rel} value (%) in the case of the same front or rear suspension system in the two cases of carrying 01 and 02 people is similar in trend in the speed regions. The TR_{rel} value in the front and rear suspension systems does not exceed the allowable deformation limit in the entire speed range v and ξ_s. Considering the same value of ξ_s, in the front suspension system, when carrying 01 person, according to the increasing direction of the vehicle speed v, the TR_{rel} value increases and reaches a maximum at the speed v = 70 (km/h), outside this speed region, the TR_{rel} value decreases. When the vehicle carries 02 people, the TR_{rel} value reaches a maximum at v = 50 (km/h) and decreases when v>50 (km/h). Considering the same value of v, as increasing the value of ξ_s the TR_{rel} value decreases and reaches a minimum at ξ_s = 0.8. For the rear suspension system, considering the same value of ξ_s, as the vehicle speed increases, the TR_{rel} value gra–dually increases and reaches its maximum at the vehicle speed values v_{max}; this v_{max} value increases as the ξ_s value decreases. The optimal ξ_s value of the rear sus–pension system is the maximum surveyed ξ_s value. Considering the response to the vertical dynamic load TR_{TDL} (%) at the wheels, in the surveyed speed region, the TR_{TDL} value (%) is always greater than the static load value, so the wheel's road grip decreases as the vehicle speed increases when going over bumps. The optimal ξ_s value is distributed irregularly in the surveyed speed region. For the front wheel, in the case of 01 people sitting, in the speed range v<30 (km/h), the optimal ξ_s value decreases from 0.8 to 0.2 and remains unchanged in the speed range 30 (km/h)<v<50 (km/h), in the speed range 50 (km/h)<v<70 (km/h) the optimal ξ_s value gradually increases to 0.8 and remains un–changed when the vehicle speed increases. For a vehicle carrying 02 people in the low-speed range v<30 (km/h), the optimal ξ_s value is below 0.2; outside this speed range, the optimal ξ_s value is the maximum surveyed ξ_s value.

Harmonic excitation

Similar to the time domain response survey with transient excitation, the typical response value over time with harmonic excitation was also obtained in 02 cases, Figure 10. Accordingly, in the first case with excitation frequency value f = 1 (Hz), the acceleration response of a vehicle carrying 02 people is always greater than that of 01 people. In addition, when the vehicle carries the same number of people, the acceleration response with ξ_s = 0.2 and ξ_s = 0.5 are approximately the same. This trend is valid for the cases of relative displacement response in the front and rear suspension systems. In the second survey case, the response value at high-fre–quency f = 3 (Hz) is always more significant than that at low-frequency f = 1 (Hz). For the acceleration response, the case of a vehicle carrying 02 people has a lower response, and vice versa for the cases of suspension displacement response.

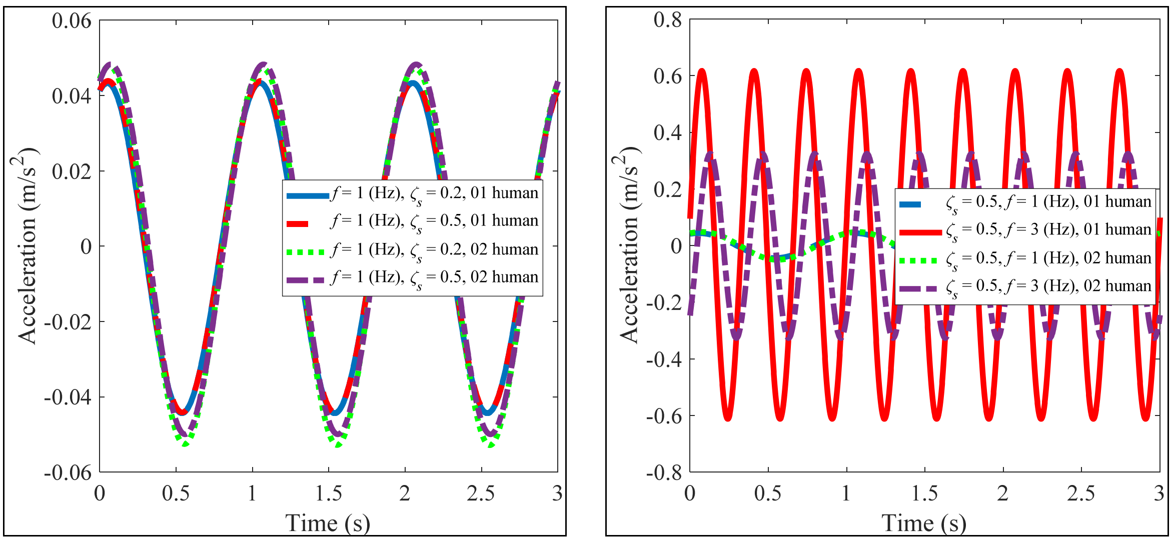

a. Acceleration (m/s²), *f* = 1 (Hz)

b. Acceleration (m/s²), ξ_b = 0.5

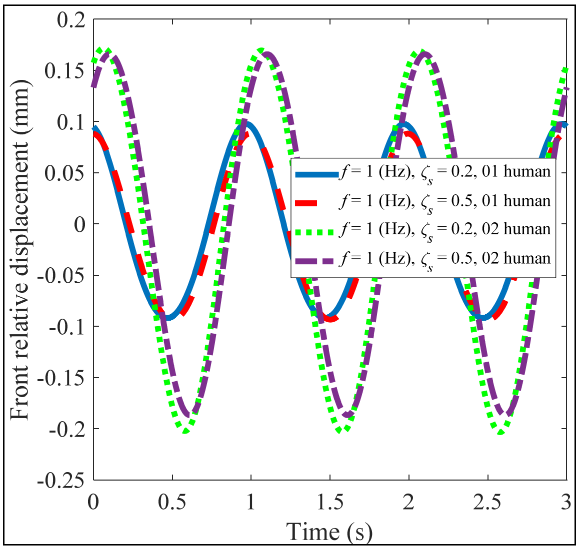

c. Front relative displacement, *f* = 1 (Hz)

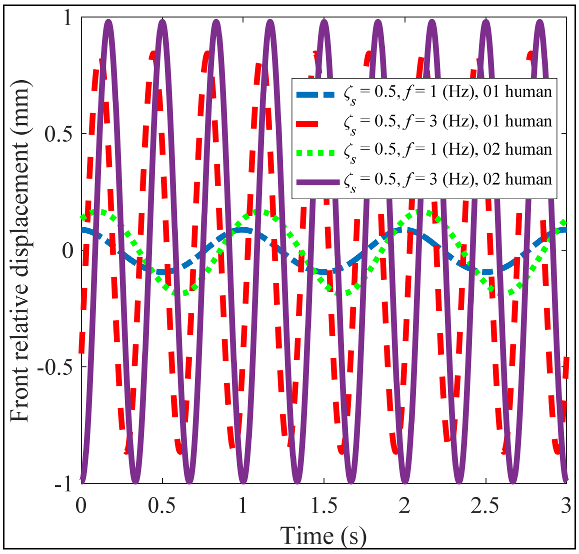

d. Front relative displacement, ξ_b = 0.5

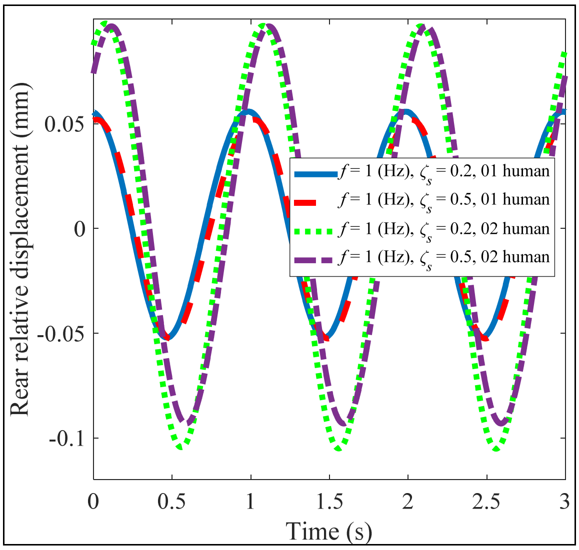

e. Rear relative displacement, *f* = 1 (Hz)

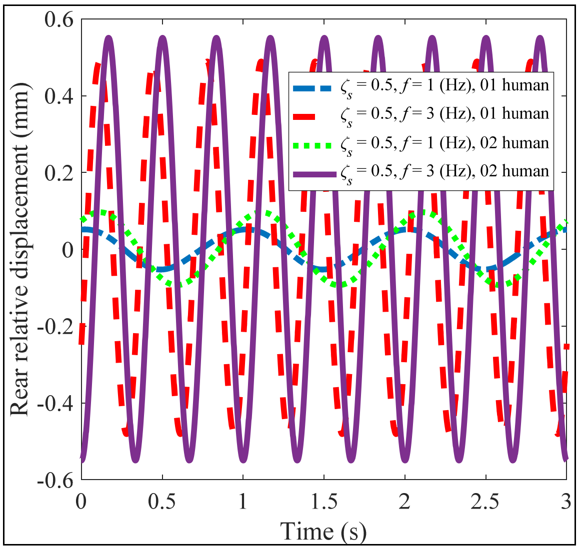

f. Rear relative displacement, ξ_b = 0.5

Figure 10. Harmonic - Responses in the time domain

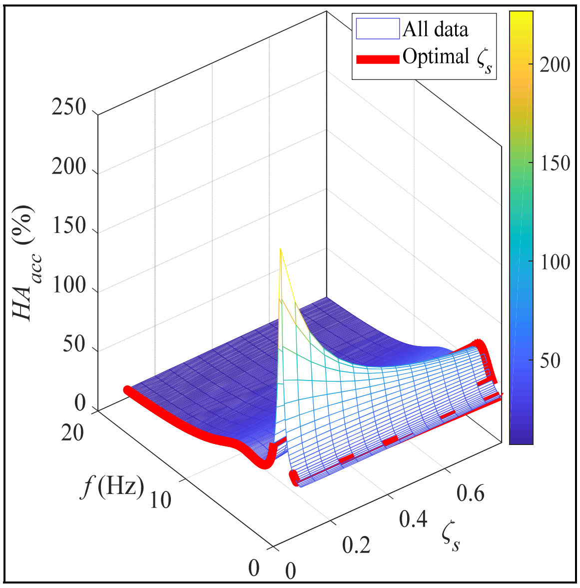

a. HA_{acc} (%) – 01 occupant

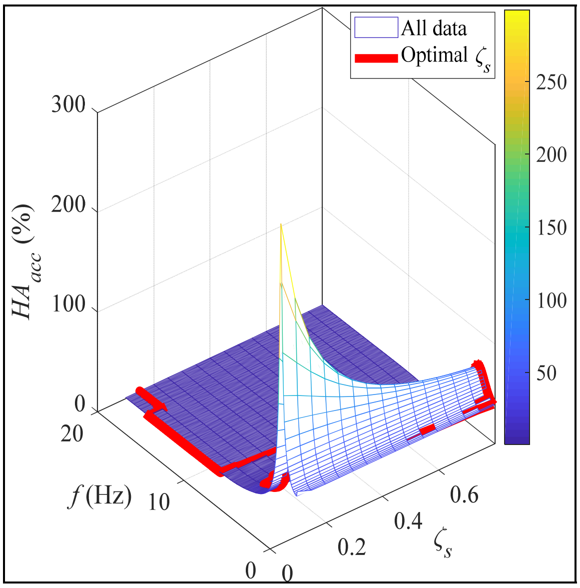

b. HA_{acc} (%) – 02 occupants

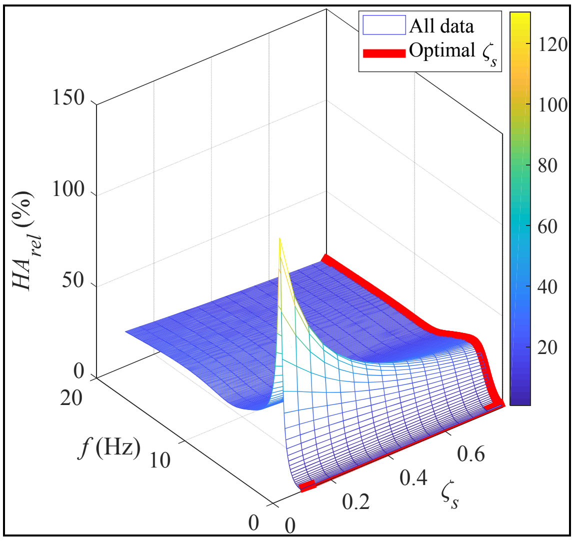

c. Front HA_{rel} (%) – 01 occupant

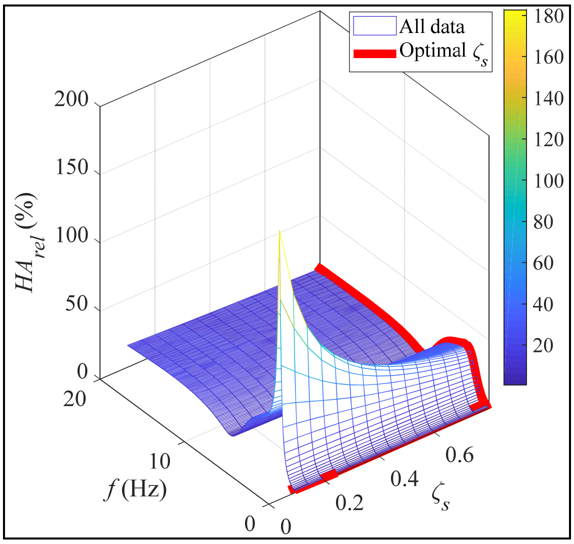

d. Front HA_{rel} (%) – 02 occupants

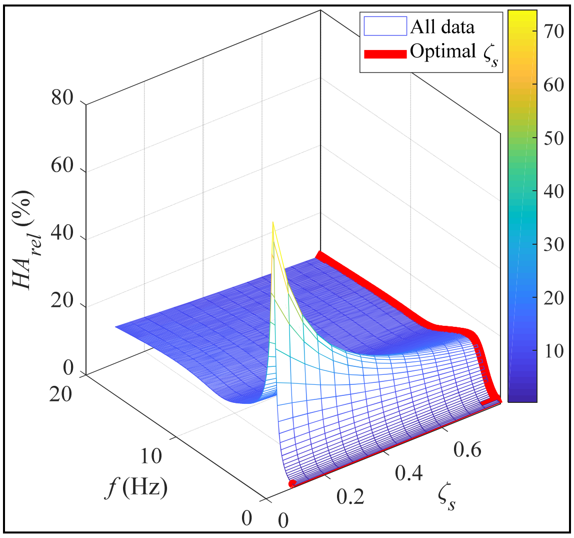

e. Rear HA_{rel} (%) – 01 occupant

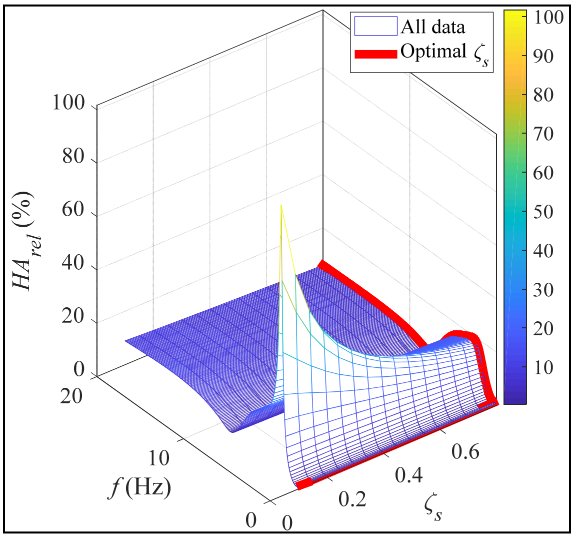

f. Rear HA_{rel} (%) – 02 occupants

Figure 11. Harmonic - Gain responses in the excitation frequency f and damping ratio ξ_b domain

When subjected to harmonic excitation, the response values in the frequency domain include the acceleration response HA_{acc} (%) and the relative displacement response HA_{rel} (%), Figure 11. For the human body acceleration response HA_{acc}, the cases of vehicles carrying 01 and 02 people have resonant frequency values at f_{re} = 2.5 (Hz) and f_{re} = 1.5 (Hz), respectively, over the entire investigated ξ_s value range. However, at the resonant frequency, as the ξ_s value increases, the resonance response amplitude decreases. In addition, in the investigated frequency domain, the optimal ξ_s value in the cases of carrying 01 and 02 people, respectively, in the frequency range $f \in$ [0.5 5] (Hz), $f \in$ [0.5 3] (Hz) is 0.8, outside this frequency range, the optimal ξ_s value is 0.2. For the relative displacement response of the front and rear suspension HA_{rel}, when the vehicle carries 01, 02 people, the optimal value of ξ_s is 0.8 over the entire frequency range. In addition, the maximum response at the resonance frequency of the front suspension is always greater than that of the rear suspension, considering the same number of people. With the same front or rear suspension, the response value at the resonance frequency when the vehicle carries 02 people is greater than that of 01 people.

Random excitation

The acceleration response values on the investigated speed domain in the case of the vehicle moving on road surface C at all ξ_s values are summarized in Figure 12, Figure 13. Accordingly, the trend of acc_v value in the speed domain and the ξ_s domain when the vehicle carries 01 and 02 people is similar. Specifically, the optimal ξ_s value in the surveyed speed domain is 0.2. In the entire vehicle speed domain, as ξ_s increases, the acc_v value decreases to a minimum at ξ_s = 0.2 and increases as ξ_s increases. In addition, in the entire ξ_s value domain, as the vehicle speed increases, the acc_v value increases. In particular, the acc_v value when the vehicle carries 01 people is larger than when carrying 02 people in the entire surveyed domain of v and ξ_s, thereby making the vehicle carrying 02 people create a better feeling when the vehicle moves on the road surface C.

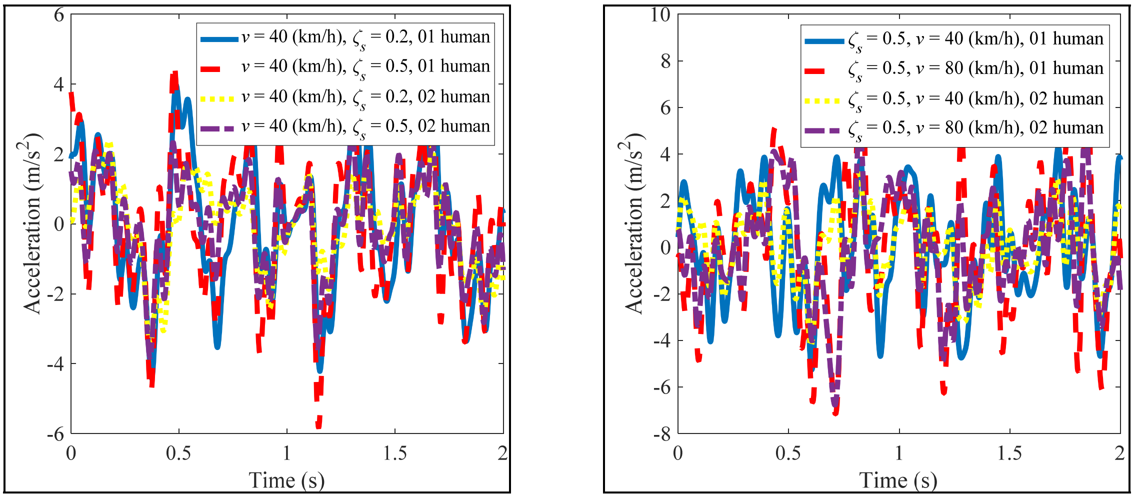

a. acc_v (m/s^2), v = 40 (km/h) **b. acc_v (m/s^2), ξ_b = 0.5**

Figure 12. Random - Responses in the time domain

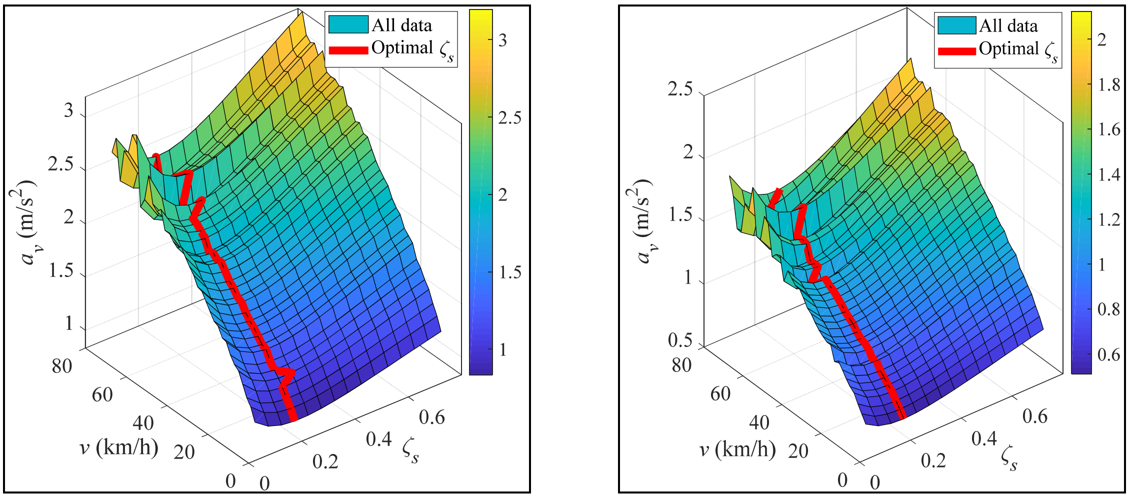

a. acc_v (m/s^2) – 01 occupant **b. acc_v (m/s^2) – 02 occupants**

Figure 13. Random - Responses in the velocity v and damping ratio ξ_b domain

5. CONCLUSIONS

The study has applied the multi-body dynamic mo–delling method to describe the electric vehicle suspen–sion system using Matlab Simscape. Through this mo–del, the study has analyzed the output responses of the driver and the suspension system when subjected to different types of excitation. The analysis results show that:

+ With transient excitation: In the working speed range, both the cases of vehicles carrying 01 and 02 people are likely to lose vertical stability when the TR_{acc} value exceeds 100% at high-speed values v>60 (km/h), the optimal ξ_s value is not distributed consistently but changing a lot with different speed ranges. In addition, the TR_{acc} response value when the vehicle carries 02 people is lower than when the vehicle carries 01 people under the same survey conditions. The response of the vehicle body pitch angle around the *Oy* axis is relatively small (<6^o); the optimal ξ_s value is mainly distributed in the high-value region ξ_s = 0.8. The response of the relative displacement of the front and rear suspension systems TR_{rel} increases with increasing speed and decreases with increasing ξ_s value of the survey. However, as TR_{rel}<100% in all surveyed cases, the relative displacement of the vehicle suspension system does not exceed the allowable limit. In addition, the TR_{rel} value reaches its minimum when the ξ_s value is the largest in the surveyed region. The response of the dynamic load at the wheel TR_{TDL} is always greater than 100% in the medium and high-speed region v>30 (km/h), so when moving over the bump in this speed region, the vehicle is at risk of losing traction.

+ With harmonic excitation: The resonance frequ–ency values of the entire suspension system when carrying 01 and 02 people are reached at f_{re} = 2.5 (Hz) and f_{re} = 1.5 (Hz), respectively. As the ξ_s value inc–reases, the resonance amplitudes of HA_{acc} and HA_{rel} decrease. With the ξ_s value <0.4, the HA_{acc} and HA_{rel} values at the resonance frequency exceed 100%. When the excitation frequency value f>5 (Hz), the HA_{acc} and HA_{rel} values decrease rapidly. The optimal ξ_s value range for HA_{acc} in the low and high-frequency regions is ξ_s = 0.8 and ξ_s = 0.2, respectively. For the HA_{rel} value, the optimal ξ_s value is in the 0.8 region.

+ With random excitation: In the entire vehicle speed range, as ξ_s increases, the acc_v value decreases and reaches a minimum at ξ_s = 0.2, then increases as ξ_s

increases. In the entire ξ_s value range, as the vehicle speed increases, the acc_v value increases. With the cur–rent suspension system, the occupant will always feel uncomfortable when moving on road surface C with $PSD\ \Phi_{0C} = 8.10^{-6}$ (m^3/rad).

ACKNOWLEDGEMENT

We acknowledge Ho Chi Minh City University of Technology (HCMUT), VNU-HCM for supporting this study.

REFERENCES

[1] Huu Nhan Tran and Ngoc Dai Pham, An investigation of the Wenda GI.34 bus driver seat based on the whole-body vibration exposure level, *International Journal of Vehicle Noise and Vibration*, Vol. 19, No. 3/4, 2023

[2] Ngoc Dai Pham, A comparison of vibration behavior of linear and nonlinear bus driver seat suspension system using the 5dof model, *FME Transactons*, Vol. 53, No. 2, pp. 196-211, 2025.

[3] Heidarian A, Wang X., Review on Seat Suspension System Technology Development. *Applied Science*, No. 14, pp. 1-20, 2019

[4] International Organization for Standardization (1997) ISO 2631-1: 1997, "Mechanical Vibration and Shock - Evaluation of Human Exposure to Whole-body Vibration. Part 1: General Requirements," Geneva, ISO.

[5] Goodarzi A., Khajepour A., *Vehicle suspension system technology and design*, Morgan & Claypool, 2017.

[6] Puhn F., *How to make your car handle*, Bill Fisher, 1976.

[7] Georg R., *Road Vehicle Dynamics: Fundamental and Modeling*, Taylor & Francis, 2012.

[8] Ngoc Dai Pham and Huu Nhan Tran, Calculation to Determine the Optimal Shock Absorber of a Bus Driver Seat's Suspension System, *GMSARN International Journal*, Vol. 19, pp. 227-236, 2025

[9] Ngoc Dai Pham, Analyzing the influences of bus driver seat's suspension system on driver's comfort level and stability, *Noise & Vibration Worldwide*, Vol. 55, No. 11, pp. 618-631, 2024

[10] Sharp R., The Influence of the Suspension System on Motorcycle Weave-mode Oscillations, *Vehicle System Dynamics: International Journal of Vehicle Mechanics and Mobility*, Vol. 5, No. 3, pp. 147-154, 1976

[11] Amrit S., David N., Motorcycle suspension design using matrix inequalities and passivity constraints, *Vehicle System Dynamics: International Journal of Vehicle Mechanics and Mobility*, Vol. 50, No. 3, pp. 377-393, 2012

[12] Liu C., Lin W., Hung C., Hwang C., Feasibility Assessments and Designs of a Hybrid Suspension System for Motorbike Application, *IEEE Transactions on Industry Applications*, Vol 53, No. 4, pp. 3420–3427, 2017

[13] Maciejewski I., Meyer L., Krzyzynski T., Mo–delling and multi-criteria optimisation of passive seat suspension vibro-isolating properties, *Journal of Sound and Vibration*, Vol. 324, pp. 3-5, 2009

[14] Cristiano S., Sergio S., Luca F., Experimental ana–lysis of a motorcycle semi-active rear suspension, *Control Engineering Practice*, Vol. 18, pp. 1239-1250, 2010

[15] L. Wu, W. Zhang, Hierarchical Modeling of Semi-Active Control of A Full Motorcycle Suspension With Six Degrees of Freedom, International *Journal of Automotive Technology*, Vol. 11, No. 1, pp. 27-32, 2010

[16] Guida, D., Pappalardo, C.: A New Control Algo–rithm for Active Suspension Systems Featuring Hysteresis, *FME Transactions*, Vol. 41, pp. 285-290, 2013.

[17] Federico B., Francesco L., Roberto R., Roberto S., and Onorino T., Electronic Control of a Motorcycle Suspension for Preload Self-Adjustment, *IEEE Transactions on Industrial Electronics*, Vol. 55, No. 7, 2008

[18] F. Baronti, F. Lenzi, R. Roncella, R.Saletti and O. DiTanna, Embedded Electronic Control System for Continuous Self-Tuning of Motorcycle Suspension Preload, *IEEE 2007 Mediterranean Conference on Control & Automation - Athens*, Greece

[19] Thomas L., Dominik S., Stefan O., and Wolfgang Steiner, Identification of a nonlinear spring and damper characteristics of a motorcycle suspension using test ride data, *PAMM*, Vol. 18, pp. 1-4, 2018

[20] The Indian Roads Congress, IRC-99-1988, Tenta–tive Guidelines on the Provision of Speed Breakers for Control of Vehicular Speeds on Minor Roads.

[21] Gillespie T. *Fundamentals of Vehicle Dynamics*, New York: SEA, 1992.

[22] International Organization for Standardization (ISO). "Mechanical vibration – Road surface pro–files – Reporting of measured data." Switzerland. Standard No. ISO 8608. ISO, 2016.

NOMENCLATURE

w_d	Standard weight of the driver	70	kg
w_p	Standard weight of the passenger	70	kg
w_{ch}	Weight of the vehicle's chassis	35	kg
w_b	Weight of the vehicle's power source	57	kg
s_f	Combination of stiffness of the vehicle's front coil springs	30000	N/m
s_r	Stiffness of the vehicle's rear coil spring	130000	N/m
s_{fw}	Stiffness of the vehicle's front wheel	140000	N/m
s_{rw}	Stiffness of the	140000	N/m

	vehicle's rear wheel		
d_f	Combination of damping coefficient of the vehicle's front dampers	--	Ns/m
d_r	Damping coefficient of the vehicle's rear damper	--	Ns/m
d_{fw}	Damping coefficient of the vehicle's front wheel	150	Ns/m
d_{rw}	Damping coefficient of the vehicle's rear wheel	150	Ns/m
y_{hf}, y_{hr}	Front and rear excitation signals from road	--	m
g	Gravitational acceleration	9.81	m/s^2
Δx_{Lf}/ Δx_{Lr}	Front and rear suspension's deformation limit	90/30	mm
w_c	Human, chassis and power source mass		
w_{uf}	Front unsprung mass		
w_{ur}	Rear unsprung mass		
I_c	Human, chassis and power source moment of inertia		
s_{eqf}	Equivalent stiffness of front suspension		
s_{eqr}	Equivalent stiffness of rear suspension		
d_{eqf}	Equivalent damping coefficient of front suspension		
d_{eqr}	Equivalent damping coefficient of rear suspension		
s_{eqfw}	Stiffness of front wheel		
s_{eqrw}	Stiffness of rear wheel		
b_1, b_2	Center of gravity position		
h_g	Height of center of gravity		
ϕ	Pitch angle		

ИСТРАЖИВАЊЕ НОВЕ ПРОЦЕНЕ ВИБРАЦИЈА ВЕШАЊА МОТОЦИКЛА КОРИШЋЕЊЕМ ДИНАМИЧКОГ МОДЕЛА СА ВИШЕ ТЕЛА НА РАЗЛИЧИТИМ ПОВРШИНАМА ПУТА

Н.Д. Фам

Ова студија је допринела новој методи у анализи вибрационих одзива вешања мотоцикла са коефи–цијентом пригушења ξ_s коришћењем динамичког модела са више тела (MBD). Посебна каракте–ристика ове методе је да MBD модел може да представи понашање система без успостављања динамичких једначина.

Ова метода захтева успос–тављање чврстих кинематичких ограничења између елемената модела у XY равни на позицијама споја као што су пут - точак, точак - вођица - вешање - оквир мотора у Matlab Simmechanics окружењу. Ре–зултати се процењују на основу различитих индекса одзива као што су убрзање, релативно померање, способност држања пута и ниво удобности у складу са случајевима рада под хармонијским, пролазним и случајним побуђењима. Одзиви MBD модела у слу–чајевима рада теже да буду у складу са стварношћу и могу се применити у процесу пројектовања вешања мотоцикла на основу процене утицаја ξ_s.